

## Section A: Using Landsat data to quantify vegetation changes in Kalimantan, Borneo

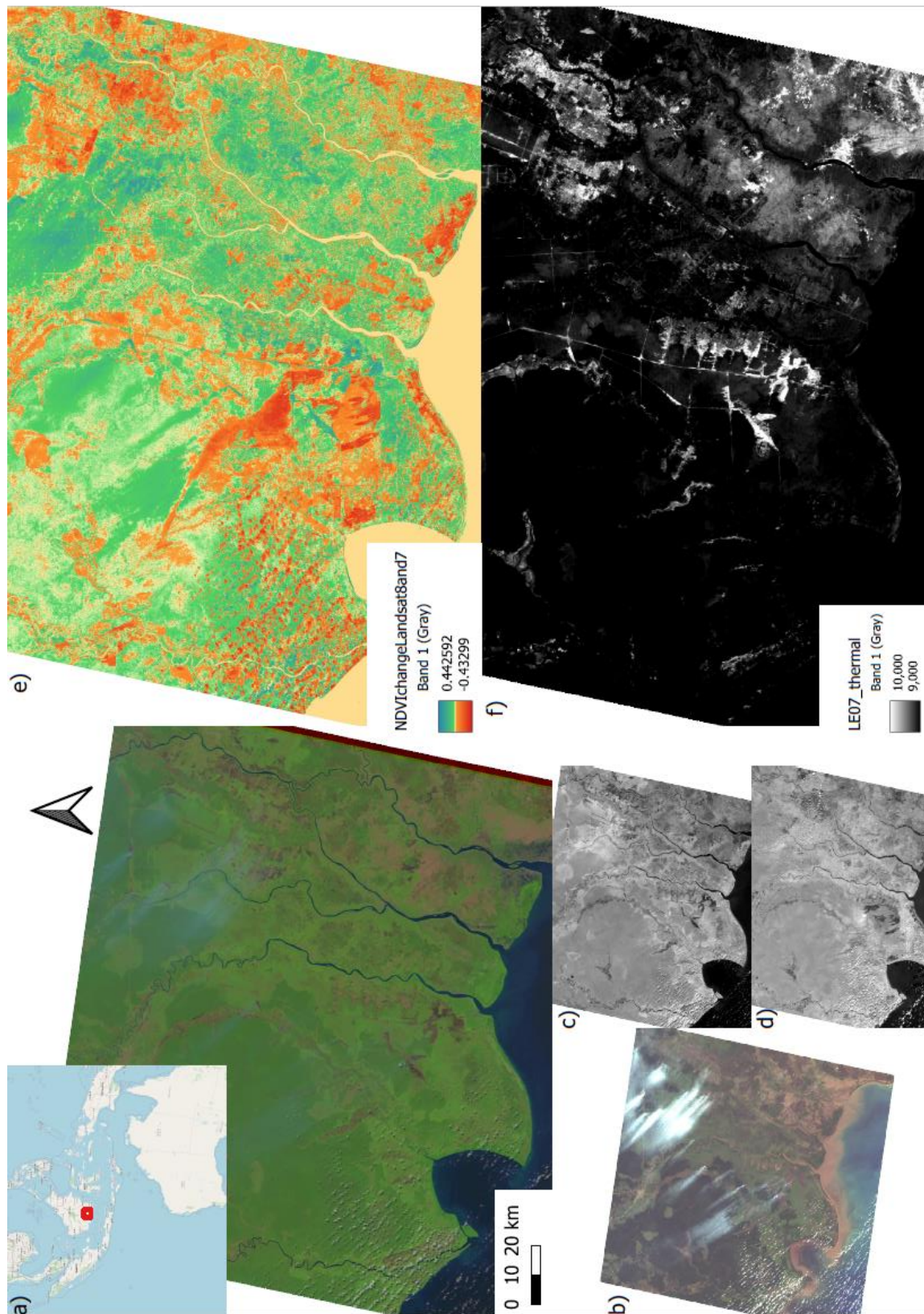


Figure 1. Vegetation change in Kalimantan, south Borneo, using Landsat 7 and 8. a) Colour image Landsat 7 (20/08/2001), b) Virtual raster (20/08/2001) c) Near infrared Landsat 7 (20/08/2001), d) Near infrared Landsat 8 (28/09/2018), e) NDVI change Landsat 7 and Landsat 8, f) Thermal Landsat 7, show the areas of increased heat due to fires and agriculture.

## Section B: Using MODIS to quantify land cover changes in Kalimantan, Borneo

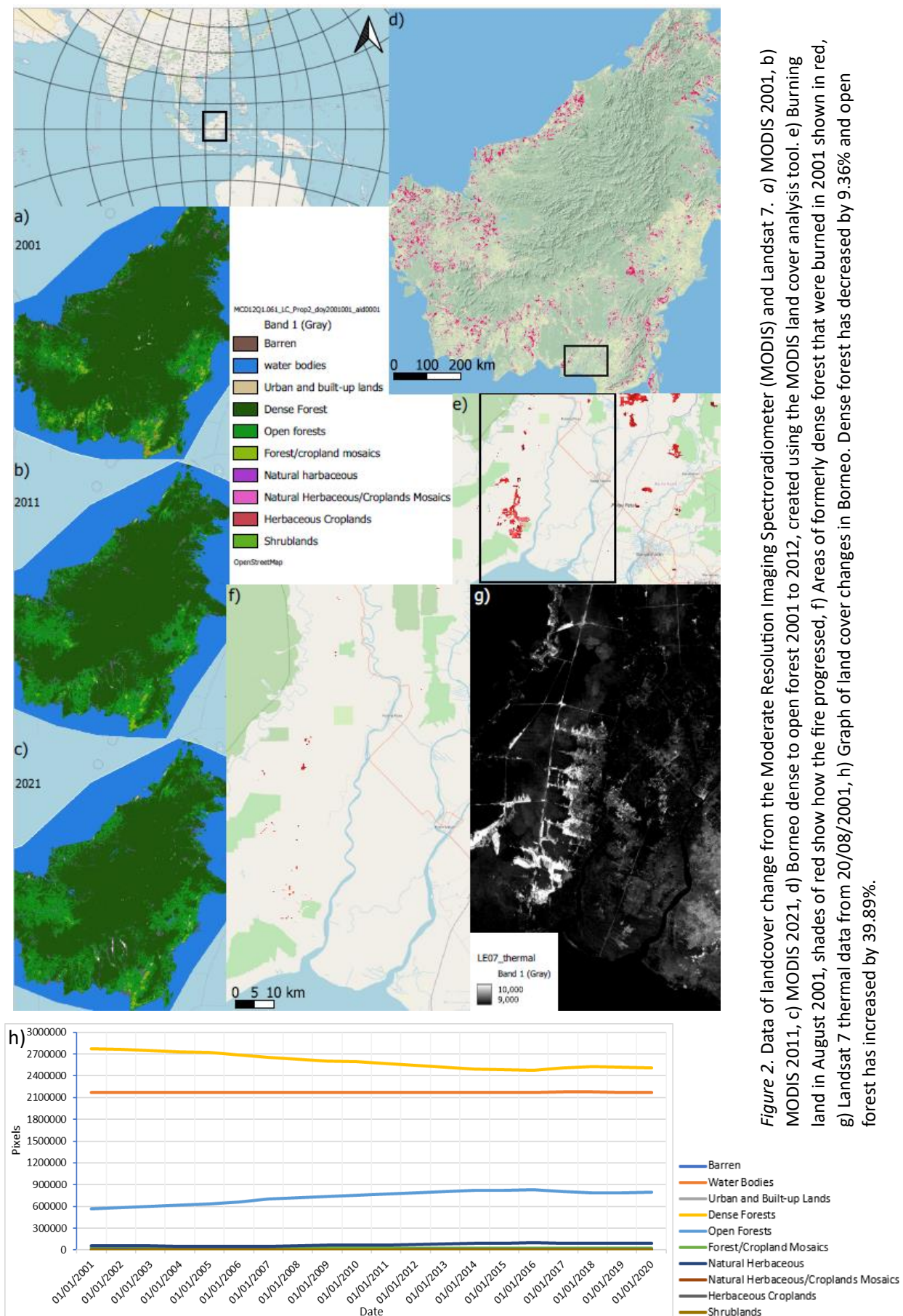


Figure 2. Data of landcover change from the Moderate Resolution Imaging Spectroradiometer (MODIS) and Landsat 7. a) MODIS 2001, b) MODIS 2011, c) MODIS 2021, d) Borneo dense to open forest 2001 to 2012, created using the MODIS land cover analysis tool. e) Burning land in August 2001, shades of red show how the fire progressed, f) Areas of formerly dense forest that were burned in 2001 shown in red, g) Landsat 7 thermal data from 20/08/2001, h) Graph of land cover changes in Borneo. Dense forest has decreased by 9.36% and open forest has increased by 39.89%.



## Section C: Using optical feature-tracking to quantify glacier flow changes.

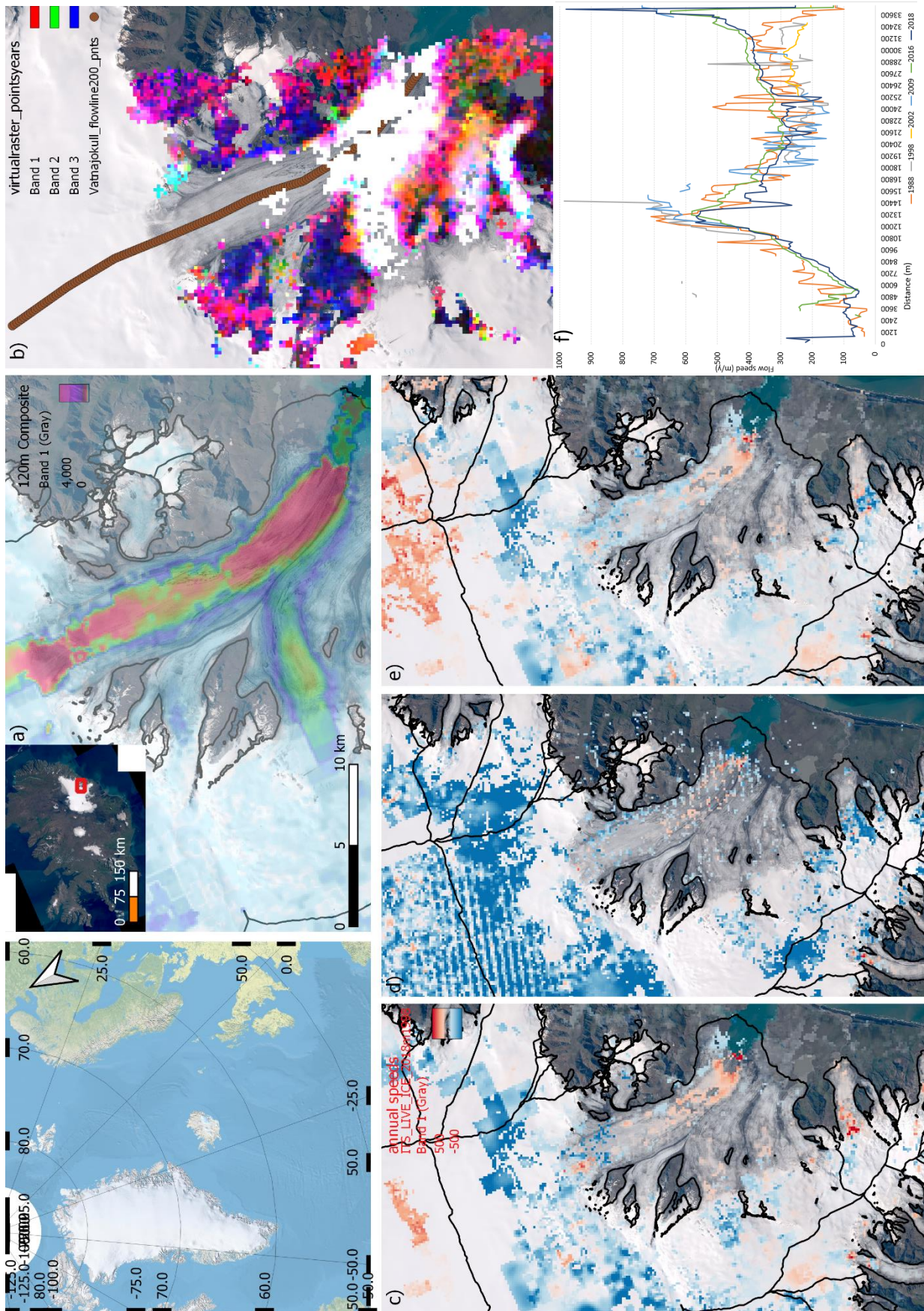


Figure 3. Optical feature-tracking analysis of the Vatnajökull glacier, Iceland, using ITS\_LIVE data. a) 120m resolution composite band, flow speed in m/year, b) virtual raster for the years 1988, 1998, 2002, 2009, 2016, and 2018, using the central flowline, c) feature tracking for flow speed variation 1988-1998, outlined in the GLIMS polygon shapefile, d) 2013-2018 feature tracking, e) 2016-2018 feature tracking, f) graph of flow speed along the central flowline, made using the attribute table. There are waves of increasing speed.

## Section D: Using the ArcticDEM and Landsat to quantify changes to the Batagaika Crater, Siberia

### 1. Introduction & rationale

The Batagaika crater lies in the Yana Upland of Northern Yakutia (Kizyakov *et al.*, 2022) in eastern Siberia. The crater gets its name from its location, being only 10km southeast of the village of Batagay in the centre of the Verkhoyansk district (Vadakkedath, Zawadzki, and Przeździecki, 2020). The continental subarctic climate (Koppen, 2011) means temperatures range from 15.5 °C in the summer to -44.7 °C in the winter (Vadakkedath, Zawadzki, and Przeździecki, 2020). Precipitation levels are low at 203mm/year (Murton *et al.*, 2017).

The Batagaika crater is the world's largest retrogressive mega thaw slump (Yanagiya *et al.*, 2023), at 0.82 km<sup>2</sup> in April 2023. The crater started as a depression in the early 1970s due to deforestation between Mount Khatyngnakh and Kirgillyakh (Vadakkedath, Zawadzki, and Przeździecki, 2020). Because of reduced shade from tree cover, there was thermo-denudational development of the depression at the end of the 1980s (Günther *et al.*, 2015). The growth of the crater expanded outwards from the position of the initial ravine (Kizyakov *et al.*, 2022) and is now characterised by a 'tail' and 'head' shape which channel out the meltwater. In some areas the walls rise 55m above the crater floor (Kizyakov *et al.*, 2022), which exposes sediment dating back to the mid-Pleistocene, marine isotope stage 1 (Kizyakov *et al.*, 2022). The crater therefore acts as a 'natural laboratory' for palaeoenvironmental research and the study of permafrost thaw in the warming Arctic climate (Kizyakov *et al.*, 2023). Retrogressive thaw slumps like this only occur in areas where there is high ground ice content (Runge *et al.*, 2022), which is therefore more responsive to changes in temperature.

The landscape of Northern Yakutia is shaped by permafrost degradation processes (Günther *et al.*, 2015, Nace, 2017), which occur when the ice-rich yedoma deposit reaches thermal disequilibrium and goes above 0°C (Murton *et al.*, 2017). The yedoma deposit is a 7-20m thick Pleistocene age permafrost that contains 50-90% ice (Kunisky *et al.*, 2013); even a slight perturbation in temperature has a large impact on the ice content. The area is already showing signs of thaw (Ivanova *et al.*, 2013), in that thermokarst landscapes now cover 20% of the northern permafrost region (Olefeld *et al.*, 2016). Depressions are occurring due to subsidence, from cryogenic slope processes, which form thermokarst landscapes (Holloway *et al.*, 2020, Khomutov *et al.*, 2017); this is also occurring in coastal regions (Kizyakov *et al.*, 2022). The soils are becoming more saturated and boggy, which destabilises the soil and causes trees to collapse. This can clear a whole forest to create a thermokarst bog. Once the permafrost melts more, bog becomes inundated, forming a thermokarst lake, which are now abundant in northern Siberia (Khomutov *et al.*, 2017). Most thermokarst lakes are only a few metres deep, but some can reach up to 40m deep (Soare *et al.*, 2007). During this process, carbon is released from the soils and into the atmosphere; this adds to global greenhouse gas concentrations.

The Batagaika crater will be quantified since 2000 using the ArcticDEM (PGC, 2023), Advanced Spaceborne Thermal Emission and Reflectance Radiometer Global DEM (ASTER) (ASTER, 2019) on the Terra satellite (Abrams and Crippen, 2019) and Landsat 7-9 (USGS, 2023). The study will look at the patterns of the thaw slump expansion, due to temperature and vegetation. The results of this study can be extrapolated to other ice rich deposit regions to understand how climate change is impacting permafrost melt at a wider scale and in the future.

## 2. Data & Methods

Analysis was undertaken in QGIS 3.30.1 with an 84 / NSIDC Sea Ice Polar Stereographic North (EPSG: 3413) map projection. Like Vadakkedath, Zawadzki, and Przeździecki (2020), data was from the spring or summer (April-August) as this is when melt and temperature are at their greatest.

### 2.1 The ArcticDEM

ArcticDEM (PGC, 2023) strip index for years 2012, 2017 and 2021 (PCG, 2023) and ASTER (ASTER, 2019) for 2000 digital elevation models were analysed to quantify volume changes. The DEMs were converted into hillshades and differenced to display the elevation changes between the years, with ASTER data being 'warped' to fit the new map projection. The volume of the most recent crater was calculated using the zonal statistics tool with a differenced DEM raster layer. From the attribute table values, volume change was calculated.

$$volume\ change\ (km^3) = \frac{sum\ of\ pixels \times mean\ of\ elevation\ change}{10^9}$$

DEMs are created through the active remote sensing technique of photogrammetry, whereby multiple images are taken of the earth's surface to gain a 3D image. The spatial resolution for the ArcticDEM is 2m (PGC, 2023) and 15m for ASTER (Abrams and Crippen, 2019). This is the minimum distance two objects must be apart to be identified individually. It can therefore be expected that the ArcticDEM images will be clearer and more accurate. The ArcticDEM is made of individual stereoscopic DEMs which extract from pairs of Maxar satellite imagery. In comparison, the ASTER DEM is compared to other remote sensing data and any masking errors from cloud cover are filled with an alternative DEM (Abrams and Crippen, 2019).

### 2.2 Landsat

Landsat level 2 data was used as it does not include interference from atmospheric particles, such as clouds, which cause scattering due to the water droplets being longer than the wavelength. This is corrected in Landsat 8 & 9 with band 9 (cirrus) (GISGeography, 2022). The crater's area was digitised and calculated for each year (Table 1).

The normalised differenced vegetation index (NDVI) was used to compare photosynthesis within the crater. The NDVI calculation used Landsat 8's Operational Land Imager (OLI) bands 4 (Red) and 5 (NIR). Vegetation reflects strongly in the NIR and low for Red, hence NDVI shows the location of high NIR reflectance. Only 2017 and 2021 were differenced, as Landsat 9 data was still undergoing processing (USGS, 2023), and Landsat 7's scan line error caused outputs to not be uniform when comparing years.

$$NDVI = \frac{(NIR - Red)}{(NIR + Red)}$$

Landsat 7 ETM+ (band 6), and Landsat 8 & 9 TRIS (bands 10 and 11) (USGS, 2023), display thermal reflectance patterns, indicating the areas of highest ground temperature.

## 3. Results

Since 2005 the Batagaika crater's area has expanded by 223.43% (Fig. 4a-c). The largest expansion has been along the western and southern walls. The rate of expansion has maintained somewhat stable with an increase between 2017 and 2021 (Table 1).

Date	Satellite	Area (km <sup>2</sup> )	Annual area increase from previous date (km <sup>2</sup> /year)
26 <sup>th</sup> June 2005	Landsat 7 ETM+	0.367	n/a
16 <sup>th</sup> August 2012	Landsat 7 ETM+	0.567	0.028
17 <sup>th</sup> June 2017	Landsat 8 TRIS and OLI	0.625	0.015
20 <sup>th</sup> July 2021	Landsat 8 TRIS and OLI	0.777	0.038
16 <sup>th</sup> April 2023	Landsat 9 TRIS-2 and OLI-2	0.820	0.022

*Table 1.* Area and annual area increase of the Batagaika crater between 2005 and 2023.

Between 2017 and 2021 there were areas with positive NDVI (Fig. 4d), concentrated around the west and southern part, and upper 'tail'.

DEM data shows widening of the crater, most noticeably the 'tail' of the crater (Fig. 6). This is the same location of the highest thermal reflectance values (Fig. 5), with high thermal values in June 2005 and July 2012 (Fig. 5a, and 5d). For 2000, in Figure 6, the crater is poorly visible due to the low resolution of the ASTER GDEM dataset (Fig. 6a). The 2021 data shows the crater with a flatter western wall and larger area than the 2012 Landsat data (Fig. 6d) due to the cloud removal algorithm failing to remove all cloud cover from the dataset during processing (Fig. 7c). This is discounted as true elevation change.

The crater expansion is outwards with a decrease in the elevation of the surrounding walls (Fig. 7). There is minimal elevation decrease in the centre that occurs in 2000-2012. Throughout the study period the crater's volume decreased by 1.033 km<sup>3</sup> (Fig. 7d), averaging to 0.049 km<sup>3</sup>/year.

2000-2012 the volume decrease was 0.623 km<sup>3</sup> (figure 7, a), and during 2012-2021 it decreased by 0.029 km<sup>3</sup>. This averages to 0.052 km<sup>3</sup>/year for 2000-2012, and 0.003 km<sup>3</sup>/year for 2012-2021, so the rate of volume change has decreased.



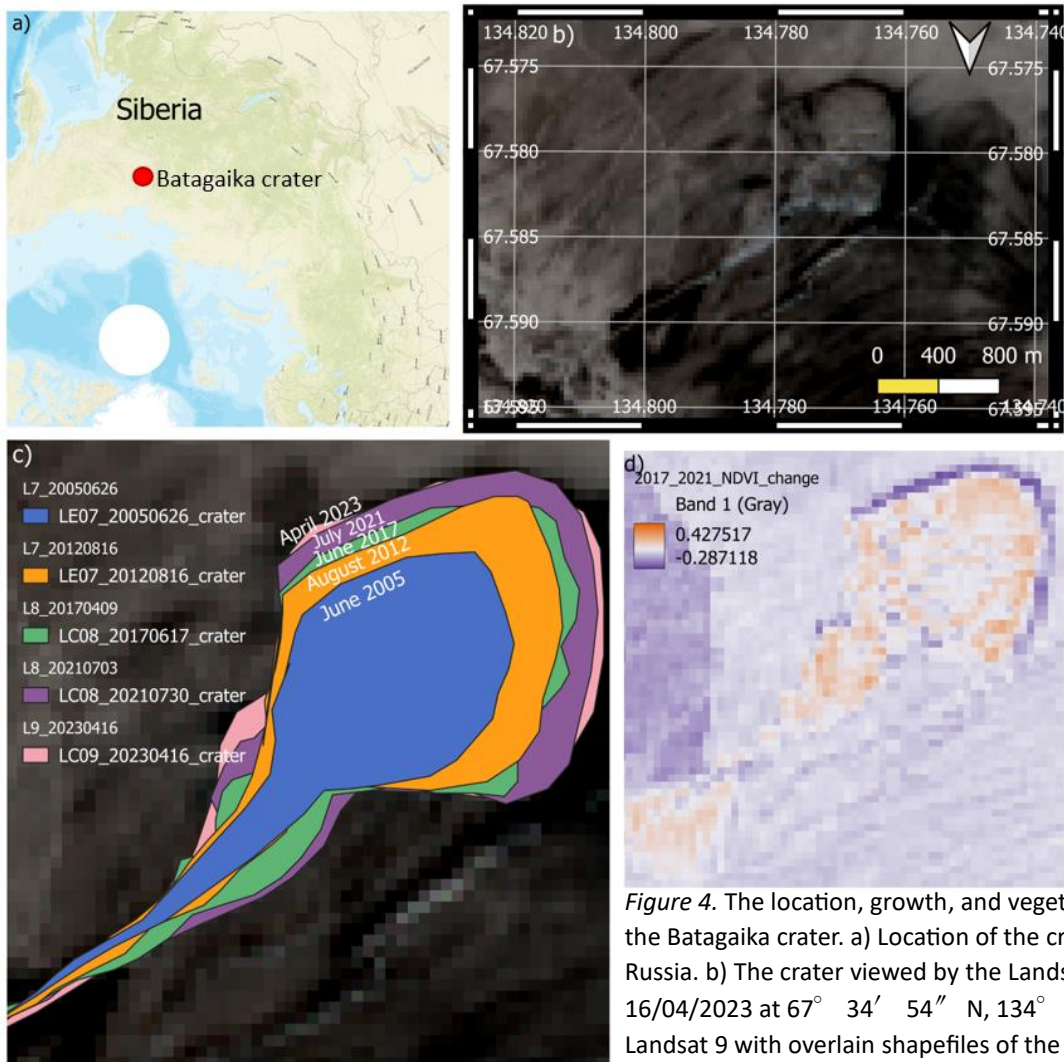


Figure 4. The location, growth, and vegetation patterns of the Batagaika crater. a) Location of the crater in Siberia, Russia. b) The crater viewed by the Landsat 9 from 16/04/2023 at 67° 34' 54'' N, 134° 46' 44'' E c) Landsat 9 with overlain shapefiles of the digitised crater from 26/06/2005, 16/08/2012, 17/06/2017, 30/07/2021 and 16/04/2023. d) NDVI calculation of differenced years 2017 and 2021 using Landsat 8 bands 4 and 5.

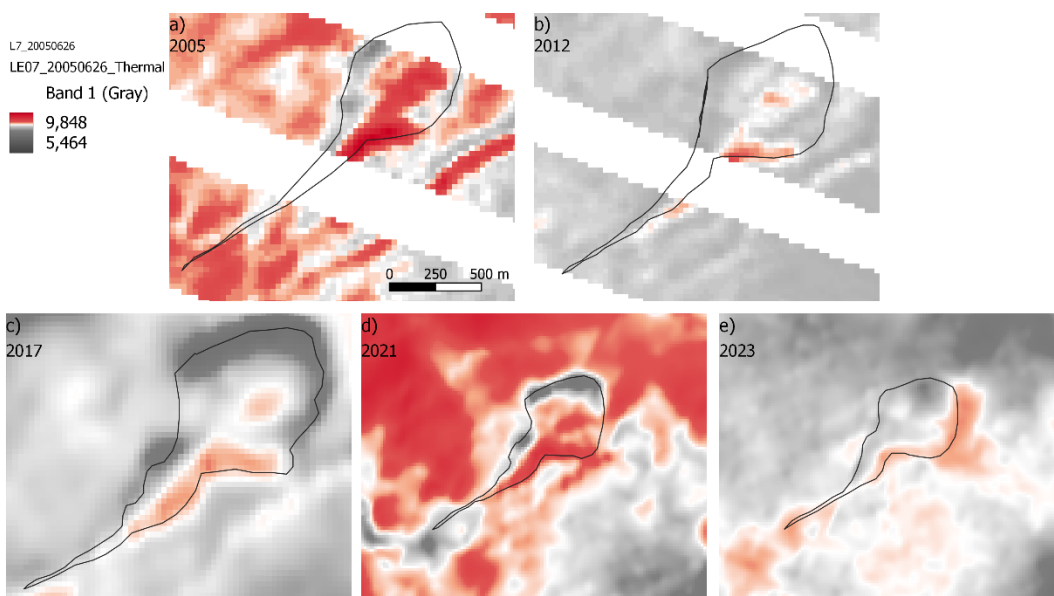


Figure 5. Thermal reflectance of the crater from Landsat level 2, band 6 for Landsat 7, and bands 10 and 11 for Landsat 8 & 9. a) 26/06/2005. b) 16/08/2012. c) 17/06/2017. d) 30/07/2021. e) 16/04/2023.

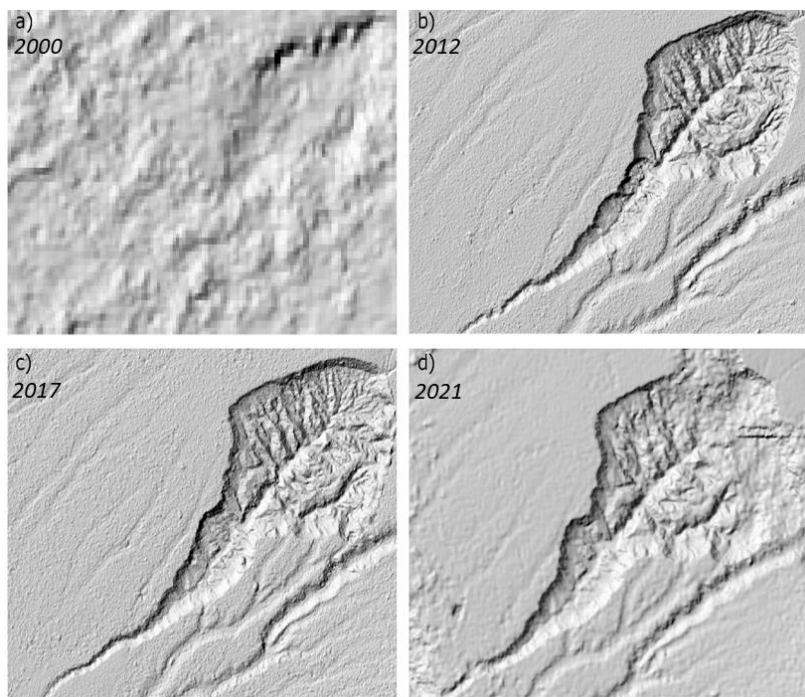


Figure 6. Digital elevation model (DEM) hillshade of the Batagaika crater from 2000 to 2021. a) ASTER Global DEM 2000. b) ArcticDEM 18/05/2012. c) ArcticDEM 17/04/2017. d) ArcticDEM 21/05/2021

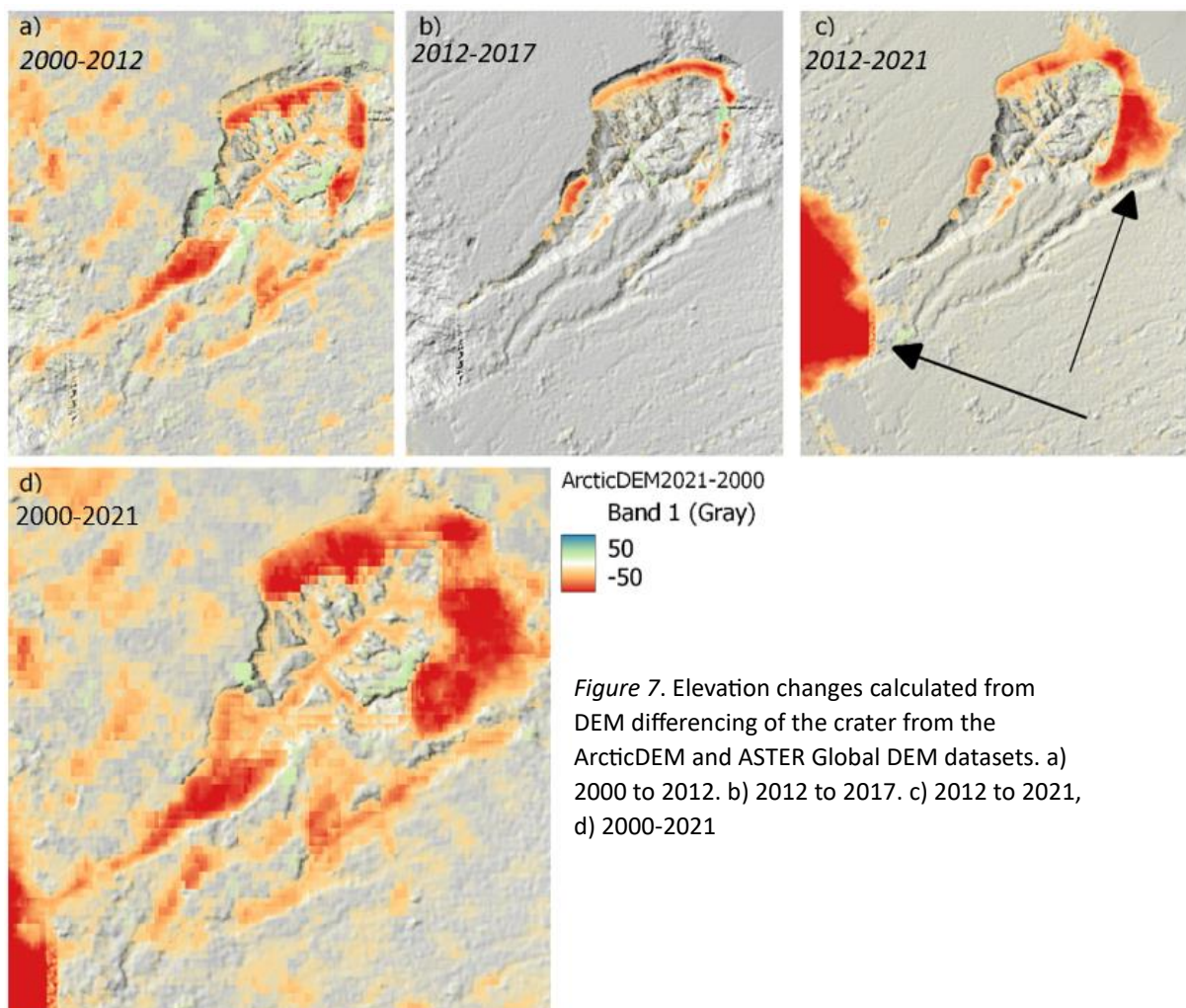


Figure 7. Elevation changes calculated from DEM differencing of the crater from the ArcticDEM and ASTER Global DEM datasets. a) 2000 to 2012. b) 2012 to 2017. c) 2012 to 2021, d) 2000-2021



#### 4. Interpretation & Discussion

Despite the Batagaika not being initially caused by climate warming, it is land surface temperature that drives its further growth (Kizyakov *et al.*, 2022; Vadakkedath, Zawadzki, and Przeździecki, 2020), with the ice being vulnerable to degradation under climate change (Babkina *et al.* 2019; Günther *et al.*, 2015; Hinzman *et al.* 2005). The warmest areas are focused on the centre, north-westerly side of the crater (Fig. 5). Vadakkedath, Zawadzki, and Przeździecki (2020) observed the centre to be the warmest part of the crater, with the southern part being the coldest. The western edge is expanding quickly; this is thought to be due to the upper ice complex, a permafrost layer containing tabular ice (Kizyakov *et al.*, 2022), being entirely exposed in this section of the crater (Günther *et al.*, 2015; Savvinov *et al.*, 2018). This wall is therefore very sensitive to temperature change. Temperatures are projected to rise twice as fast in the Arctic, compared to the rest of the planet, due to climate change (IPCC, 2021; Welch, 2019). This will increase the thaw of the western wall (Fig. 4c, Fig. 5), causing it to expand and deepen further; a recent study has already observed this to be true (Vasiliev *et al.*, 2020). The permafrost will therefore enter a positive feedback of degradation (Turesky *et al.*, 2020).

The Batagaika crater has not stabilised or experienced a decrease in its expansion (Savvinov *et al.*, 2018). Landsat shows the crater has increased by 223.43% since 2005 and has a growth rate of 0.0257 km<sup>2</sup>/year, and 0.029 km<sup>3</sup>/year since 2000. This is only different by <1m<sup>2</sup> to the observations made by Vadakkedath, Zawadzki, and Przeździecki (2020) between 1991 and 2018 with an increase of 0.026 km<sup>2</sup>/year. Yet the same study also recorded the area of the crater to be 0.780 km<sup>2</sup> in June of 2018 (Vadakkedath, Zawadzki, and Przeździecki, 2020), compared to the crater only being measured at 0.777 km<sup>2</sup> in 2021 in this study. This difference is most likely due to the 30m spatial resolution of Landsat data (Butler, 2013), causing ambiguity when identifying the definite edge of the crater. Despite the seemingly level rate of expansion, Khomutov *et al.* (2017) argue that the enlargement rate of thaw slumps slows down with an increase in their total area. Between 2021 and 2023 the annual area increase was 0.022 km<sup>2</sup>, less than the years prior, but this is because the crater had only experienced one summer melt season, due to the 2023 data being in April. Detailed volume analysis of every year since the early 1980s would need to be done to gain a complete understanding of the Batagaika crater's growth to determine if its expansion has slowed.

The Batagaika crater has an overall positive NDVI, with some areas experiencing an increase of 0.427 between 2017 and 2021 (Fig. 4d), showing vegetation succession inside the crater. A general increase since 2010 was also found by Vadakkedath, Zawadzki, and Przeździecki (2020), who put forward that this reduces the melting of permafrost due to their findings of a slowdown in expansion rate from 2014-2018 compared to 2010-2014, similar to the observed decrease in volume expansion in this study. Afforestation and maintaining forest cover would be an option to minimising permafrost melt at a wider scale.

Permafrost in the northern circumpolar region is a huge sink of carbon, storing 1,460 to 1,600 Pg of soil organic carbon (Schuur *et al.*, 2018), double the amount of carbon that is in the atmosphere (Turesky *et al.*, 2020). The permafrost climate feedback is identified as one of the largest feedbacks due to climate change (Ciais *et al.*, 2013; Koven *et al.*, 2011). This means that the widescale permafrost melt in Northern Yakutia, and Siberia is of great significance. The development of thaw slumps in the Yedoma district is due to forest clearance and wildfires (Günther *et al.*, 2015). This has caused erosional ravines to form in the locations of deforestation, this is similar to how the Batagaika crater began (Ivanova, 2003; Savvinov *et al.*, 2018). With climate change and anthropogenic impacts, thaw slumps are becoming larger and more common (Khomutov *et al.* 2017). The Batagaika crater therefore represents a fraction of the thaw slumps and the potential for carbon release.

## References

- Abrams, M., and Crippen, R. (2019) 'ASTER GDEM V3 (ASTER Global DEM)', User Guide Version 1, *California Institute of Technology. U.S.*, Available at: [https://lpdaac.usgs.gov/documents/434/ASTGTMTM\\_User\\_Guide\\_V3.pdf#:~:text=Each%20ASTER%20GDEM%20tile%20has%20two%20associated%20files%3A,edge%20row%20and%20column%20in%20the%20adjacent%20cell](https://lpdaac.usgs.gov/documents/434/ASTGTMTM_User_Guide_V3.pdf#:~:text=Each%20ASTER%20GDEM%20tile%20has%20two%20associated%20files%3A,edge%20row%20and%20column%20in%20the%20adjacent%20cell) (Accessed: 22/04/2023)but
- Butler, K. (2013) 'Band Combinations for Landsat 8', ESRI ArcGIS Blogs, 24/07. Available at: <https://www.esri.com/arcgis-blog/products/product/imagery/band-combinations-for-landsat-8/#:~:text=Here%E2%80%99s%20how%20the%20new%20bands%20from%20Landsat%208,0.53%20%E2%80%93%200.59%20%208%20more%20rows%20> (Accessed: 22/04/2023).
- Esri. "Standard" basemap, Scale Not Given, available at: <https://qms.nextgis.com/geoservices/510/>. (Accessed: 18/04/2023).es
- GISGeography (2022) 'Landsat 8 Bands and Bands Combinations', GISGeography, Available at: <https://gisgeography.com/landsat-8-bands-combinations/> (Accessed: 22/04/2023)
- Günther, F., Grosse, G., Wetterich, S., et al. (2015) "The Batagay mega thaw slump, Yana Uplands, Yakutia, Russia: permafrost thaw dynamics on decadal time scale," *EPIC3PAST Gateways - Palaeo-Arctic Spatial and Temporal Gateways - Third International Conference and Workshop*, Potsdam, Germany, 2015-05-18-2015-05-22 Potsdam, TERRA NOSTRA - Schriften Der GeoUnion Alfred-Wegener-Stiftung [Preprint].
- Ivanova, R. N. (2003) 'Seasonal thawing of soils in the Yana River valley, northern Yakutia'. In: Phillips M, Springman SM, Arenson LU (eds) *Permafrost, proceedings of the eighth international conference on permafrost*, 21–25 July 2003, Zurich, Switzerland, pp 479–482
- Khomutov, A., Leibman, M., Dvornikov, Y., Gubarkov, A., Mullanurov, D., Khairullin, R., (2017) "Activation of Cryogenic Earth Flows and Formation of Thermocirques on Central Yamal as a Result of Climate Fluctuations," in *Springer eBooks*. Springer Nature, pp. 209–216. Available at: [https://doi.org/10.1007/978-3-319-53483-1\\_24](https://doi.org/10.1007/978-3-319-53483-1_24).
- Kizyakov, A. I., Wetterick, S., Günther, F., et al. (2022) "Landforms and degradation pattern of the Batagay thaw slump, Northeastern Siberia", *Geomorphology*, 420, p. 108501. Available at: <https://doi.org/10.1016/j.geomorph.2022.108501>
- Köppen W (2011) 'The thermal zones of the earth according to the duration of hot, moderate and cold periods and to the impact of heat on the organic world', translated by: Volken E, BrönnimannS. *Meteorol Z*, 20:351–360
- Murton, J.B., Edwards, M.E., Lozhkin, A., Anderson, P, M., Savvinov, G, N., Bakulina, N., Bondarenko, O, V., Cherepanova, M, V., Danilov, P, P., Boeskorov, V., Goslar, T., Grigoriev, S., Gubin, S, V., Korzun, J, A., Lupachev, A, V., Tikhonov, A., Tsygankova, V, I., Vasilieva, G, V., and Zanina, O, G. (2017) 'Preliminary paleoenvironmental analysis of permafrost deposits at Batagaika mega slump, Yana Uplands, northeast Siberia', *Quaternary research*, 87(2):314–330
- NASA (2022) *Landsat 9*. Available at: <https://landsat.gsfc.nasa.gov/satellites/landsat-9/> (Accessed: 22/04/2023)



NASA/METI/AIST/Japan Spacesystems and U.S./Japan ASTER Science Team (2019). 'ASTER Global Digital Elevation Model V003 year 2000', NASA EOSDIS Land Processes DAAC, available at <https://doi.org/10.5067/ASTER/ASTGTM.003> (Accessed: 17/03/2023)

Polar Geospatial centre (PGC) (2023) *ARCTIC DEM*. Available at: <https://www.pgc.umn.edu/data/arcticdem/> (Accessed: 22/04/2023)

Soare, R, J., Kargel, J, S., Osinki, G, R., Costard, F. (2007) "Thermokarst processes and the origin of crater-rim gullies in Utopia and western Elysium Planitia," *Icarus*, 191(1), pp. 95–112. Available at: <https://doi.org/10.1016/j.icarus.2007.04.018>.

USGS (2023) *Landsat 9*. Available at: <https://www.usgs.gov/landsat-missions/landsat-9> (Accessed: 22/04/2023)

USGS, Science for a changing world, Collection 2 Landsat 7 Enhanced Thematic Mapper Plus (ETM+) Level-2 Science Product, <https://earthexplorer.usgs.gov/>, data from 2005/06/26, 2012/08/16. DOI: /10.5066/P9C7I13B (Accessed: 18/04/2023)

USGS, Science for a changing world, Collection 2 Landsat 8-9 OLI (Operational Land Imager) and TIRS (Thermal Infrared Sensor) Level-2 Science Product, <https://earthexplorer.usgs.gov/>, data from 17/06/2017, 07/30/2021, 16/04/2023. DOI: /10.5066/P9OGBGM6 (Accessed: 18/04/2023)

USGS, Science for a changing world, Landsat 7 Enhanced Thematic Mapper Plus (ETM+) Collection 2 Level-1 15- to 30-meter multispectral data, <https://earthexplorer.usgs.gov/>, data from 2005/06/26, 2012/08/16. DOI: /10.5066/P9TU80IG (Accessed: 18/04/2023)

USGS, Science for a changing world, Landsat 8-9 Operational Land Imager (OLI) and Thermal Infrared Sensor (TIRS) Collection 2 Level-1 15- to 30-meter multispectral data, <https://earthexplorer.usgs.gov/>, data from 17/06/2017, 07/30/2021, 16/04/2023. DOI: /10.5066/P975CC9B (Accessed: 18/04/2023)

Vadakkedath, V., Zawadzki, J. and Przeździecki, K. (2020) "Multisensory satellite observations of the expansion of the Batagaika crater and succession of vegetation in its interior from 1991 to 2018," *Environmental Earth Sciences*, 79(6). Available at: <https://doi.org/10.1007/s12665-020-8895-7>

Welch, C. (2019) 'Arctic Permafrost is thawing fast. That affects us all', *National Geographic*, Available at: <https://www.nationalgeographic.com/environment/article/arctic-permafrost-is-thawing-it-could-speed-up-climate-change-feature> (Accessed: 03/03/2023)

Yanagiya, K. Furuya, M., Danilov, P., Iwahana, G. (2023) "Transient Freeze-Thaw Deformation Responses to the 2018 and 2019 Fires Near Batagaika Megaslump, Northeast Siberia," *Journal of Geophysical Research: Earth Surface*, 128(2). Available at: <https://doi.org/10.1029/2022jf006817>